

## Attracting Fingers with Waves

### Potential Fields Using Active Lateral Forces Enhance Touch Interactions

Cai, Zhaochong; Abbink, David; Wiertlewski, Michaël

**DOI**

[10.1145/3706598.3714030](https://doi.org/10.1145/3706598.3714030)

**Licence**

CC BY

**Publication date**

2025

**Document Version**

Final published version

**Published in**

CHI '25: Proceedings of the 2025 CHI Conference on Human Factors in Computing Systems

**Citation (APA)**

Cai, Z., Abbink, D., & Wiertlewski, M. (2025). Attracting Fingers with Waves: Potential Fields Using Active Lateral Forces Enhance Touch Interactions. In N. Yamashita, V. Evers, K. Yatani, X. Ding, B. Lee, M. Chetty, & P. Toups-Dugas (Eds.), *CHI '25: Proceedings of the 2025 CHI Conference on Human Factors in Computing Systems* Article 925 ACM. <https://doi.org/10.1145/3706598.3714030>

**Important note**

To cite this publication, please use the final published version (if applicable).

Please check the document version above.

**Copyright**

Other than for strictly personal use, it is not permitted to download, forward or distribute the text or part of it, without the consent of the author(s) and/or copyright holder(s), unless the work is under an open content license such as Creative Commons.

**Takedown policy**

Please contact us and provide details if you believe this document breaches copyrights.  
We will remove access to the work immediately and investigate your claim.



# Attracting Fingers with Waves: Potential Fields Using Active Lateral Forces Enhance Touch Interactions

Zhaochong Cai

Delft University of Technology  
Delft, Netherlands  
z.cai-1@tudelft.nl

David Abbink

Delft University of Technology  
Delft, Netherlands  
d.a.abbink@tudelft.nl

Michaël Wiertlewski

Delft University of Technology  
Delft, Netherlands  
m.wiertlewski@tudelft.nl

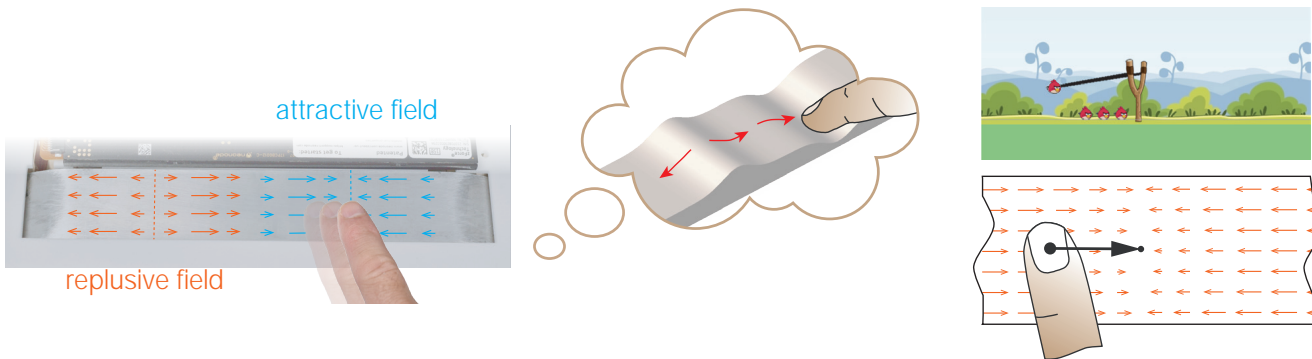


**Figure 1:** We implemented potential field rendering on a touchpad by tuning the traveling wave ratio to vary active forces. These forces are modulated based on the user's movements. By building attractive and repulsive fields (left), the surface is not perceived as a flat but a wavy surface with bumps and holes (middle). These bumps and holes can be used to create numerous haptic effects, such as a slingshot (right), basins of attraction, icons, keyboards, toggle switches, and paths for haptic guidance. In user studies, we found positive impacts of rendered potential fields during touch interactions in both users' performance and experience.

## Abstract

Touchscreens and touchpads offer intuitive interfaces but provide limited tactile feedback, usually just mechanical vibrations. These devices lack continuous feedback to guide users' fingers toward specific directions. Recent innovations in surface haptic devices, however, leverage ultrasonic traveling waves to create active lateral forces on a bare fingertip. This paper investigates the effects and design possibilities of active force feedback in touch interactions by rendering artificial potential fields on a touchpad. Three user studies revealed that: (1) users perceived attractive and repulsive fields as bumps and holes with similar detection thresholds; (2) step-wise force fields improved targeting by 22.9% compared to friction-only methods; and (3) active force fields effectively communicated directional cues to the users. Several applications were tested, with user feedback favoring this approach for its enhanced tactile experience, added enjoyment, realism, and ease of use.

## CCS Concepts

• Human-centered computing → Haptic devices; User studies.

## Keywords

Haptic feedback, surface haptics, active force, targeting task

### ACM Reference Format:

Zhaochong Cai, David Abbink, and Michaël Wiertlewski. 2025. Attracting Fingers with Waves: Potential Fields Using Active Lateral Forces Enhance Touch Interactions. In *CHI Conference on Human Factors in Computing Systems (CHI '25)*, April 26–May 01, 2025, Yokohama, Japan. ACM, New York, NY, USA, 13 pages. <https://doi.org/10.1145/3706598.3714030>

## 1 Introduction

Touchscreens and touchpads are increasingly replacing traditional mechanical buttons, dials, and sliders in human-machine interfaces. Their programmability offers a wide range of intuitive interactions with visual elements, such as tapping to select, pinching to zoom, and swiping to scroll. However, their operations can be arduous because they lack the haptic feedback of their mechanical counterparts. Without mechanical feedback, users cannot engage their reflexive sensorimotor loops for automatic manipulation that tactile and proprioceptive inputs offer. As a consequence, these interactions rely heavily on visual attention, which is impractical for visually impaired individuals and can be dangerous in situations that require continuous situational awareness, such as driving or flying.

Haptic feedback on touch panels can effectively reduce visual demand and enhance interactions. The common way to implement haptic feedback in consumer devices is to use vibrotactile actuators. The distinct vibration patterns they create inform users of a



This work is licensed under a Creative Commons Attribution 4.0 International License.  
*CHI '25, Yokohama, Japan*  
© 2025 Copyright held by the owner/author(s).  
ACM ISBN 979-8-4007-1394-1/25/04  
<https://doi.org/10.1145/3706598.3714030>

message or confirm users' operation, such as tapping or reaching a target [19]. However, the transient stimuli has limited expressiveness. A new class of devices broadly called surface haptics can provide continuous quasi-static feedback by modulating the friction between a surface and a fingertip through ultrasonic levitation [21] or electroadhesion[4]. By making the friction high on virtual targets and low everywhere else, studies have shown that users can reach targets 10% faster [9, 21, 42]. More complex patterns, such as sine waves, have shown to be useful. For example, by gradually changing the spatial wavelength of friction-modulated texture, these devices can assist users in setting a value for temperature control [5]. A similar method was used to render shapes, such as bumps or holes, on flat surfaces by mapping the local gradients of the 3D features to the friction level [18]. Despite these clear benefits, a major limitation still exists. Friction modulation only reacts against the movement of a finger due to its passivity. Thus it is only effective when the user is moving along the path of guidance. The technology fails to guide the finger in a direction other than the ongoing one. To guide users toward an arbitrary-located target, we must provide users' fingers with continuous directional forces.

Recent developments in surface haptics have demonstrated that active lateral forces could be directly applied to a user's fingertip [8, 12, 40, 41]. Contrary to friction modulation, these techniques can modify the magnitude and direction of the force acting on a fingertip, so that they can both resist and push their movements. For now, the literature has been focused on characterizing the force generation with only a few studies validating its effectiveness on users, which are edge following [11] and event-based feedback, i.e. button clicks simulation [7, 14, 17, 38]. Since the 90s, "virtual fixtures" and artificial potential fields have had successful implementations in enhancing users' operation and yielded some haptic guidance principles [29, 32]. These principles could potentially be adapted to fingertip guidance using active surface haptics. While several works showcased the potential field rendering with active forces feedback, they are limited to simple demonstrations of force-position functions [11, 12, 40]. To date, these guidance principles on touch surfaces remain untested in users, and their design possibilities are unexplored.

Here, to investigate the effects of artificial potential fields on users, we implement an impedance control scheme on a traveling wave-based active force feedback touchpad, the Ultraloop [8]. We create elastic potential fields that can attract and repulse the fingertip by actively modulating these lateral forces based on finger position. These lateral forces are controlled by tuning the phase shift and amplitude of the traveling waves. We compute the potential fields as the local negative gradients of the topography that should be felt. We ran three human-factor experiments implementing separate potential fields to evaluate the effectiveness of the method. First, we investigated whether participants could perceive the magnitude and type of macroscale shapes like bumps and holes, rendered by Gaussian-shaped potential fields. Results showed that participants can detect bumps and holes with a sensory threshold of 30 mN. Second, we evaluated user's performance in a Fitts' pointing task. When the target was presented with a step-change attraction force field around a high friction zone, users improved their speed by 22.9% to varying friction alone. In addition, we demonstrated that potential fields could convey a sense of direction to a static

user. Lastly, we designed three applications exploiting the results of the aforementioned quantitative studies to evaluate user subjective experience. These applications include (1) a haptic keyboard, which is the combination of potential wells and bumps, (2) an Angry Birds game in which users can feel the intensity and direction of the pulling sensation from a slingshot, and (3) a three-digit lock game where users can quickly locate the password under the guidance of active force field. Users' responses to a subjective questionnaire show that all these applications provide a high level of enjoyment, reduced visual engagement, and increased realism.

In summary, we implemented programmable elastic potential field rendering for fingertip guidance by controlling ultrasonic traveling waves. We validated that the rendering has positive impacts on users in three-fold:

- (1) Differentiable shape rendering, including bumps and holes, which can be applied to virtual keyboards.
- (2) Improved performance in pointing tasks, which are fundamental for navigating icons.
- (3) Simulation of physical interactions, such as the pulling sensation of an elastic slingshot.

For the first time, our results demonstrate the various benefits of active force feedback, making it a promising approach to revolutionize touch interactions toward effortless control of complex machines using fingertips and support eyes-free interaction.

## 2 Related Work

### 2.1 Haptic guidance in classical force feedback

Salisbury et al. introduced the idea of *artificial potential fields* in haptic rendering [32]. In this approach, a scalar field is constructed with artificial "hills" representing obstacles and "valleys" representing attractors. These potential fields are used to guide or constrain users to move along desired paths or avoid obstacles. These early studies suggested that imposing force as the negative gradients of potential fields could provide passive contact surfaces for three-dimensional virtual bodies. However, the design of these fields, in general, was left as an open question.

Ren et al. later proposed a potential function based on a generalized sigmoid function, which offers an intuitive way to adjust the affected area and abruptness of the potential field near the edges of protected zones [27]. In a catheter insertion task, for example, this model created a protective potential field with lower values at the vessel center and higher values near the vessel walls. Experimental results showed that the generated potential fields were sufficient to ensure obstacle avoidance while maintaining the responsiveness necessary for realistic feedback in haptic rendering. Additionally, the sigmoid function model was applied to render a simulated gear selector lever for automotive applications [15].

### 2.2 Surface haptics rendering

When touchscreens and touchpads have taken over the market, the haptic landscape has evolved, moving beyond traditional force feedback devices to new rendering methods, such as vibrotactile and surface haptics. The latter, surface haptics devices (SHDs), can provide continuous force feedback on a user's finger by modulating

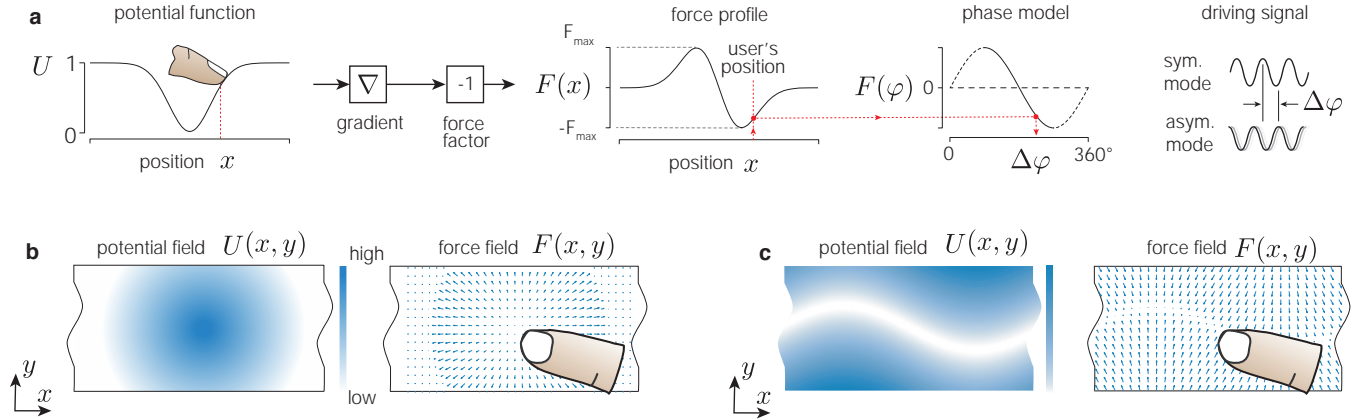


Figure 2: Visualization of potential field rendering for a bare finger in a one- (a) and two-dimensional case (b, c).

friction, either via ultrasonic lubrication, which reduces friction [36–38], or via electroadhesion, which increases friction [2, 4, 34].

Both technologies are effective in changing lateral force on a bare finger in motion across the screen. By rendering high friction on a target and low friction elsewhere, these techniques can enhance targeting performance by 7–9% compared to visual feedback alone [9, 21, 42]. Additionally, surface haptics can simulate the perception of macro shapes, such as bumps or dips, by mapping frictional forces to the gradient of height maps [3, 10, 18, 25, 31].

Despite their effectiveness, they are passive and cannot act on a static finger or push in a direction misaligned with the user's motion. Active force feedback is therefore essential to produce forces in arbitrary directions or to act on a resting finger.

### 2.3 Active lateral force on surfaces

A new family of SHDs that can generate net shear forces has recently emerged. One approach uses a moving overlay on top of a touchscreen to drag the finger to move [30]. The finger actually contacts the film and moves with it as a whole, thereby being used for conveying gesture messages to users through proprioception rather than for tactile rendering. Instead of moving the entire touch surface, net tangential forces can be generated directly on a static touch surface via oscillation, enabling users to interact with bare fingertips. Two principles have been explored.

The first principle relies on creating an asymmetry of friction by synchronizing a high or low frictional state with periodic in-plane oscillations. The frictional can be modulated through ultrasonic standing waves [11, 23, 40, 41] or electroadhesion [1, 24]. In-plane oscillations are preferably produced using ultrasonic compressive modes [40] to avoid audible noise; however, this results in nodal lines where tactile sensation is absent. The SwitchPad overcomes this limitation by dynamically switching resonant modes based on user position, achieving a uniform force profile of up to 250 mN [41], though with more complex control.

The second principle produces net lateral forces through periodic surface elliptical motions. Devices such as the LateralPad [12] and 2MoTac [14] create elliptical movements by exciting standing waves

in both longitudinal and transverse directions. Alternatively, flexural traveling waves can also produce elliptical surface motions [33], as seen in rotary traveling motors, which generate strong pushing sensations on the fingertip [6]. However, the shape of motors is not suitable for a rectangular touchpad format. In a straight beam, traveling waves can be generated by superimposing two adjacent bending modes, resulting in modest forces of 100 mN on a finger [16]. The Ultraloop, used in this work, superimposes two degenerate bending modes with identical resonant frequencies, achieving uniform forces of 300 mN with  $\pm 3 \mu\text{m}$  vibrations on a touchpad format [8].

## 3 Building potential fields

We first briefly review the principle for rendering potential fields in one- and two-dimensional (1D and 2D) cases. We then propose the implementation of this principle by controlling the traveling wave ratio on a ultrasonic active force interface.

### 3.1 Potential field rendering principle

The rendering principle is based on creating force fields within surfaces as negative gradients of potential fields. This principle has been widely used in force feedback devices [27] and active SHDs [11, 12, 40] to create haptic illusions or guide users. Figure 2a illustrates the principle for fingertip interaction in the 1D case. The input is the current finger position  $x(t)$ . The force is determined by first calculating the derivative of the potential function  $g(x) = \nabla U(x)$ , and then scaling it by a factor such that the range of the derivative linearly maps to the range of force production. Lastly, the desired force  $F(t)$  is mapped to the force generation model to produce the driving signal. As the finger moves across the surface, the driving signal is continuously updated, typically above a rate of 1000 Hz.

For 2D rendering, the force  $F(x, y)$  is obtained by taking the gradient  $G(x, y) = \nabla U(x, y)$  and scaling it, which is then translated into control signals. This method allows for creating diverse vector fields to support a wide range of interactive experiences, such as rendering bumps (Fig. 2b, holes, basins of attractions, path sinks (Fig. 2c), or saddle points.

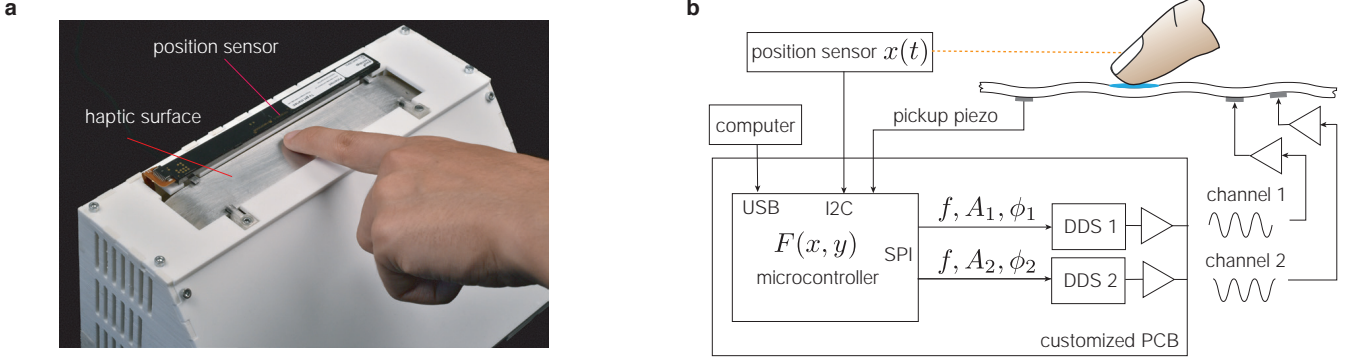


**Figure 3: Control traveling waves to render programmable potential fields.** (a) An ultrasonic traveling waves-based haptic touchpad used in this study. Users interact with the surface to experience haptic guidance or rendered objects. (b) System architecture for real-time programmable impedance rendering. Dual output channels to the haptic touchpad are updated based on finger position in real time, allowing for application-specific rendering of features (such as bumps), position-dependent friction, and impedance profiles.

### 3.2 Traveling wave-based device: Ultraloop

One necessity for the implementation of the potential field rendering is reliable and large active force generation on a relatively large flat surface. In this paper, we chose a resonant traveling wave-based device, the Ultraloop [8], and developed it for our study. The disclosed Ultraloop has a ring-shaped aluminum cavity, with a  $140 \times 30 \text{ mm}^2$  flat upper surface for touch interaction. The length-to-radius ratio of the ring is designed as 2.8 to satisfy the requirement for degenerate modes. These two degenerate standing wave modes, corresponding to the 24<sup>th</sup> order, have orthogonal spatial forms, being  $\cos(kx)$  and  $\sin(kx)$ , but share the same resonance. Their superposition with a  $\pm 90^\circ$  temporal phase shift forms a traveling wave, described mathematically as  $\cos(kx)\cos(\omega t) \pm \sin(kx)\sin(\omega t) = \cos(kx \mp \omega t)$ . The high-amplitude traveling waves induce surface elliptical motions to push fingers, with rightward force at  $90^\circ$  and leftward force at  $-90^\circ$ . As reported in [8], when the phase is not at  $\pm 90^\circ$ , partial traveling waves are generated, and the lateral force varies sinusoidally with the phase shift or traveling wave ratio, fitted by data points measured by manually tuning a function generator. This capability of uniform and large force production, combined with the feature of force varying with phase, makes the Ultraloop a strong candidate for the implementation of potential field rendering.

We replicated the aluminum cavity of the Ultraloop for force generation, using the same acoustic design as [8], and used a  $100 \times 30 \text{ mm}^2$  area for touch interaction. The ring-shaped touchpad and its control circuit are housed in a 3D-printed case, as shown in Fig. 3a.

### 3.3 Implementation of control

To control active forces in response to user movements, we employ two Direct Digital Synthesis (DDS) components (AD9834, Analog Devices, Inc.) to generate two channels of ultrasonic sine waves. These channels are synchronized with a tunable phase shift using a Teensy 3.6 microcontroller. Users movements are tracked by a position sensor (NNAMC1580PC01, Neonode) with a resolution

of 10 pixels/mm, mounted above the touch surface. The sensor communicates finger positions in x and y to the microcontroller via I2C protocol. The microcontroller, programmed using Arduino, runs an internal loop at 2000 Hz that reads the user's position, looks up the stored force profile, and generates the phase and amplitude commands for the DDS chips using the sinusoidal force-phase model. The force profiles, which are task-specific, are precomputed from the desired potential field based on the rendering principle. A graphical user interface (GUI), programmed in Python, displays the visuals of the interaction task or applications and communicates the computed force profile to the microcontroller via USB. This process allows for dynamic updates of the displayed potential fields when switching to different interaction tasks.

To identify the resonant frequency, we monitor the vibration amplitude using a piezoelectric sensor attached to the lower plate, which has been calibrated with a Laser Doppler vibrometer. An initial frequency sweep is conducted around 39425 Hz to fine-tune the resonant frequency by identifying the peak output from the piezoelectric sensor. The frequency tracking ensures a consistent vibration intensity over time. The frequency, amplitude, and phase shift data are encoded and sent to the DDSs via the SPI bus to generate corresponding sine waves. The signals (max.  $\pm 3.3 \text{ V}$ ) are amplified 20-fold (PD400, PiezoDrive) to actuate piezoelectric elements bonded to the aluminum plate. The tailored touchpad produces  $\pm 2.1 \mu\text{m}$  vibration with  $\pm 3.3 \text{ V} \times 20$  input voltages at a resonance of 39425 Hz. A diagram of this implementation is shown in Fig. 3b.

## 4 Study 1: Shape detection thresholds

In this experiment, we examine whether users could discriminate the type and amplitude of virtual bumps and holes created by repulsive and attractive potential fields.

### 4.1 Study design

To simulate the sensations of bumps and holes, we implemented repulsive and attractive potential fields from Gaussian functions. These Gaussian potential functions had an identical width  $\delta$  of 24

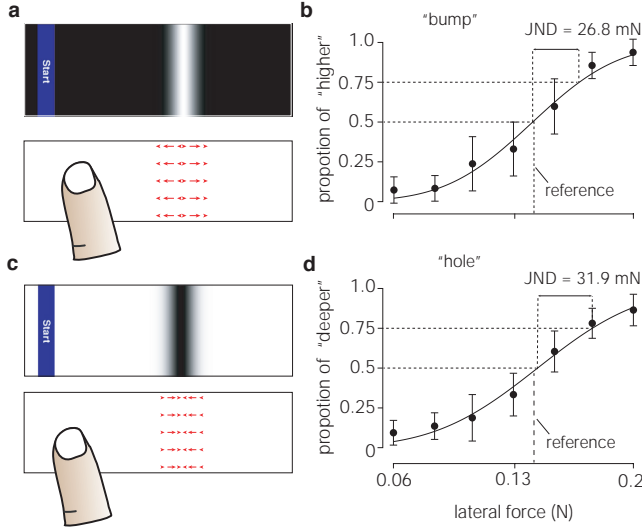


**Figure 4: (a, c) Top: graphical user interface; Bottom: force field. (b, d) Response proportion for detecting "bump" (b) or "hole" (d) as a function of active lateral force, with error bars showing standard deviations. The 75% just-noticeable difference thresholds are indicated.**

pixels and different amplitudes ( $A = 1, 0.88, 0.77, 0.65, 0.52, 0.42$ , and  $0.30$  for the experimental group;  $A=0.71$  for the reference) as shown in Fig. 4 a and c. The gradients of these Gaussian functions were linearly translated into lateral forces, such that the Gaussian with  $A = 1$  corresponded to the maximum force output ( $F_{max}$ ) and the Gaussian with  $A = 0.71$  corresponded to  $0.71F_{max}$ . These forces were then mapped to phase shifts using the data-driven force-phase model presented in Fig. 2a.

The experiment followed a two-alternative forced choice protocol. During each trial, participants were presented with two potential fields and asked to select the one perceived with higher amplitude. Each comparison consisted of the reference shape ( $A = 0.71$ ) (the mean of the experimental fields  $A = 0.77$  and  $0.65$ ) and one of the seven experimental fields. The order of the two stimuli was randomized, and participants were unaware of which was the reference. Stimuli were presented at the same location on the touchpad to ensure consistent force generation. Participants used the "Ctrl" key to switch between the two stimuli.

Each participant completed two experimental blocks: one containing repulsive potentials and the other containing attractive potentials. Each block included 56 comparison pairs ( 7 amplitudes  $\times$  8 repeats). The order of the blocks and the pairs within each block were shuffled.

**Participants.** Twelve participants (6 females and 6 males, aged 22-30, all right-handed) were recruited. All reported no sensory impairments or skin conditions. All the user studies in this paper were approved by the Ethical Committee Board.

**Experimental procedure.** Participants were seated in a chair with the haptic interface in front of them. Their arms rested comfortably on an armrest and they interacted using the index finger of their dominant hand. Participants wore headphones playing

pink noise to mask any device-related sounds. A GUI displayed the visuals of the potential fields and recorded participants' selections. Before starting the experiments, the touchpad was cleaned, and participants sanitized their fingers using alcohol wipes. These procedures were also applied to other studies in this paper.

During each trial, participants used a keyboard to make their selections: pressing "A" to choose the first and "S" to choose the second stimulus in a trial, and "Ctrl" to toggle between the two stimuli. There were no restrictions on the number of toggles, but participants were encouraged to make selections promptly.

Before the amplitude discrimination task, we conducted a pilot study to examine participants' perception of the type of the shapes. In this study, participants were presented with seven randomly selected experimental stimuli and asked to classify each as a "bump" or a "hole." Results showed that all repulsive potentials were identified as "bumps" and all the attractive ones as "holes."

## 4.2 Results

Figure 4b and d illustrate the response rate of participants for perceiving experimental stimuli as more intense than the reference (i.e. a higher bump or a deeper hole). Both the detection for "bump" and "hole" follows a typical sigmoidal shape of a psychometric curve. Stimuli with amplitudes significantly different from the reference ( $A = 1.0, 0.88, 0.42$ , and  $0.30$ ) were detected with high accuracy ( $> 78.3\%$ ), while stimuli closer to the reference ( $A = 0.65$  or  $0.52$ ) were detected with lower accuracy ( $60.3\%$ ), which is close to a  $50\%$  rate expected by chance. A fitted profit function in the psychometric model reveals points of equivalence at  $A = 0.704$  for bump detection and  $A = 0.721$  for hole detection. The 75% just-noticeable difference (JND) is  $26.8$  mN for bump and  $31.9$  mN for holes.

Participants also provided subjective feedback after completing the experiment. Most of them found that the sensations of touching a "bump" or a "hole" were trivial to differentiate. Two described the perception of bump as "first climbing up a hill and then down a slope", with the reverse sensation for "holes". Another participant noted that he/she identified a "bump" by "feeling my finger decelerating before accelerating". Additionally, two participants mentioned that detecting "holes" was slightly more challenging, and required more time to make a decision, aligning with the higher JND observed for holes.

The well-fitted sigmoidal curves in the psychometric model, combined with subjective comments, confirm that the Gaussian potential fields rendered by active force can be effectively perceived as "bumps" and "holes" by users. This discrimination ability suggests this approach could be applied to the design of tangible interfaces, such as tactile icons or keys of a keyboard.

## 5 Study 2: Fitts' Pointing task

Sliding on a touchpad to move the cursor to an icon, dragging and dropping or scrolling an alarm clock can be considered a pointing task to a desired location, which is elemental in human-computer interactions. Here, we investigate whether adding active force feedback during sliding can improve users performance in Fitts' pointing task.

## 5.1 Study design

A one-dimensional pointing task was designed, requiring participants to slide against the touchpad to locate a target using sensory cues. We used a repeated within-subjects design with three independent factors: feedback condition, target distance, and target width. A GUI displayed the task.

We evaluated user performance across four feedback modalities: active force, friction modulation, vision-only, and vision combined with active force, see Fig. 5. In the first two haptic-only conditions, targets were invisible, requiring participants to recognize them solely through touch. The last two conditions had visible targets, allowing us to assess whether adding active force feedback improves pointing performance.

For *friction modulation*, we employed a step-wise friction profile, with high friction in the target and low friction elsewhere, similar to prior studies [9, 21, 42]. Friction modulation was actuated with two standing-wave modes that are in phase. In *active force* and *vision + active force* conditions, a step-wise force profile was applied: outside the target, a uniform lateral force was used to direct the finger toward the target; while inside the target, the touchpad was deactivated to produce a high friction area as in *friction modulation*. In the *vision* condition, friction was uniformly low to eliminate any friction-induced feedback. The amplitude of driving voltages remained constant at  $\pm 66$  V across all conditions.

We tested three target distances (200, 400, and 600 pixels) and three target widths (16, 32, and 48 pixels). The control-to-display ratio was set to 10 pixels/mm, meaning the smallest and farthest target was 1.6 mm wide and 60 mm far on the touchpad. The ratio is comparable to standard laptop touchpads. The target sizes were chosen to reflect typical pointing tasks on touchpads. For example, 16-pixel targets represent small icons, such as a volume control in the corner of a laptop screen, while 48-pixel targets represent large icons, such as browser shortcuts on the taskbar. These combinations of distances and widths created nine movement conditions, yielding seven distinct indices of difficulty (ID) from 2.369 to 5.267, defined as  $\log_2(\frac{D}{W} + 1)$ , where  $D$  is the target distance and  $W$  is the width.

**Task.** Participants received the task sounds indicating the start and selecting actions through headphones. During each trial, they slid their index finger across the surface to locate the target as quickly and accurately as possible. The trial includes the following steps, adapted from [21]:

- (1) *Initial state.* The blue start area appears on either the left or right side of the interface randomly to prevent potential orientation bias. In *vision* or *vision + active force* conditions, the red target is also displayed.
- (2) *Trigger start.* Participants move the white cursor that represents the finger position to the start area, and hold for 0.6 s. An audible sound is heard, and the start area turns green. The clock starts.
- (3) *Slide to find.* Participants slide their finger to locate the target using haptic or visual cues. They are allowed to move back and forth over the target to confirm the target location in all conditions.
- (4) *Lift-off to select.* Participants lift their finger at the perceived target location. A sound is played to confirm the action of selection.

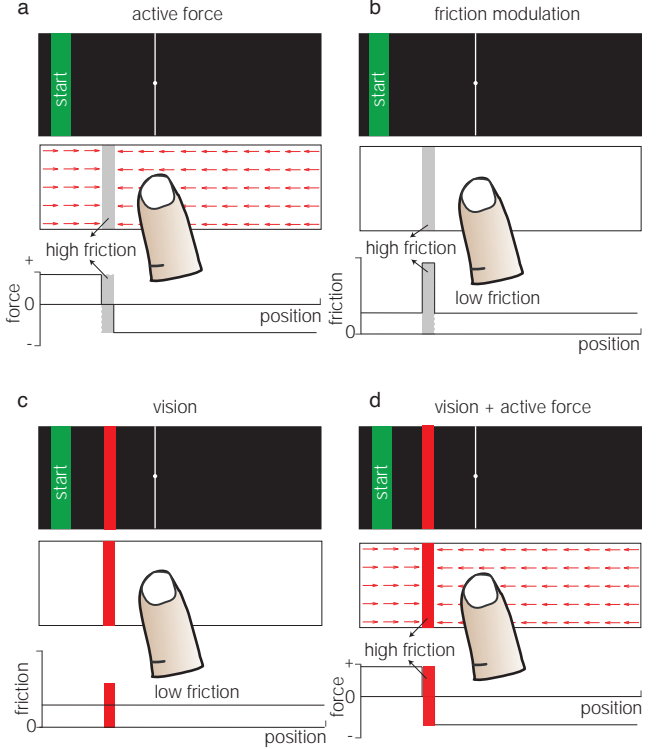


**Figure 5: Implementation of designs for force and friction profiles, evaluated as four feedback conditions in a pointing task. (a) *active force* and (d) *vision + active force* conditions share an identical force profile, where forces consistently push the finger toward the target. In (b) *friction modulation* condition, friction is high inside and low outside the target area. In (c) *vision* condition, friction remains consistently low. Targets are visible only in conditions (c) and (d).**

Participants began with a training session with the same tasks as the experimental one to familiarize themselves with the sensation and task requirements. They were encouraged to adjust the normal force applied to optimize their perception of the feedback. Training continued until participants felt familiar with the haptic sensations and task procedures but was limited to a maximum of 15 minutes per participant. After training, participants completed two experimental sessions, totaling 216 trials, including 4 feedback conditions  $\times$  3 distances  $\times$  3 widths  $\times$  6 repeats. Each session included 108 trials, with a three-minute break provided between sessions. To minimize anticipation or adaptation effects, the order of feedback and movement conditions was randomized.

**Participants.** Twelve participants (5 females and 7 males, aged 23–29, all right-handed) were recruited for this study. All reported no sensory impairments or skin ailments. None participated in S1.

## 5.2 Results

We conducted a repeated measures analysis of variance (RM-ANOVA) on four dependent variables: completion time, approach time, selection time, and entry count. The independent variables are feedback

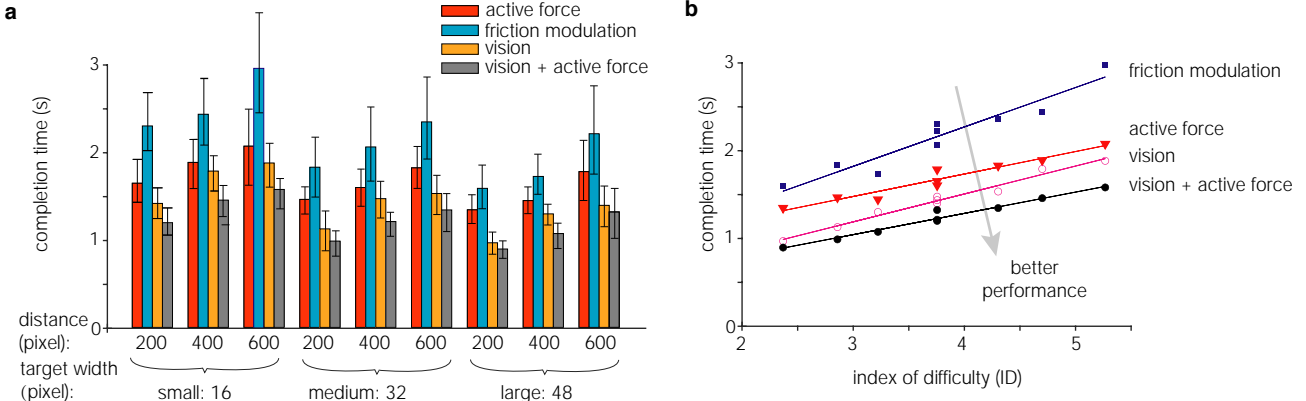


**Figure 6: (a) Mean completion time in a pointing task across nine movement conditions. (b) Linear regression for mean completion time based on Fitts' indices of difficulty (ID).**

conditions, target distances, and target widths. Additionally, we examined Fitts' law parameters and collected subjective responses from participants.

**Overall observations.** We observed that the maximum deviation between the selected and desired target position across all participants and conditions was 35 pixels ( $\approx 3.5$  mm on the touchpad). Given that this deviation is relatively small compared to the full selection range of 1000 pixels, it suggests that participants relied on sensory cues to select rather than guessing. This observation implies that both *friction modulation* and *active force* feedback provided effective cues on the presence of the target. The other observation is that the majority of extra-long trials (duration  $> 3$  s), which accounts for 3.5% of total (91 trials), occurs in *friction modulation* (82 trials), with far fewer in *active force* (8 trials) and *vision* (1 trial).

**Completion time and Fitts' law.** RM-ANOVA shows significant effects on completion time from target widths ( $F_{2,22} = 138.57, p < 0.001$ ), target distances ( $F_{2,22} = 47.545, p < 0.001$ ) and feedback modality ( $F_{3,33} = 187.63, p < 0.001$ ). Figure 6a presents the average completion times across nine movement conditions and four feedback conditions. For haptic-only conditions, *active force* required shorter completion time than *friction modulation* for all the nine movement conditions. When averaging all these movement conditions, *active force* reduced the targeting duration by 22.9 % from 2.165 s to 1.669 s, compared to *friction modulation*, with Post-hoc Tukey-Kramer tests also confirming the significant differences between them with  $p < 0.01$  across all widths and distances. These results highlight the clear advantage of active force feedback in eyes-free targeting tasks. Additionally, when combined with visual feedback, active force further reduced completion time by 15.5%, from 1.433 to 1.211 s, with post-hoc comparisons showing a significant difference between *vision* and *vision+active force* ( $p < 0.05$ ) for all movement conditions.

The Fitts' law analysis reveals a strong linear relationship between the averaged completion time and the index of difficulty across all feedback conditions (Fig. 6b;  $r^2 > 0.91$ ). The reciprocal of the slope, which represents the index of performance, highlights the notable differences between feedback modalities. For haptic-only

conditions, *active force* has a higher index than *friction modulation* (3.92 bits/s vs. 2.23 bits/s), while for visual-present conditions, *vision+ active force* outperforms *vision* (4.13 bits/s vs. 3.14 bits/s), as summarized in (Tab. 1). These comparisons demonstrate the advantages of active force feedback in both vision-present and eyes-free modalities.

| condition             | a      | b      | $r^2$ | index of performance |
|-----------------------|--------|--------|-------|----------------------|
| active force          | 0.7152 | 0.2551 | 0.939 | 3.92                 |
| friction modulation   | 0.4751 | 0.4489 | 0.915 | 2.23                 |
| vision                | 0.2337 | 0.3180 | 0.978 | 3.14                 |
| vision + active force | 0.3188 | 0.2419 | 0.970 | 4.13                 |

**Table 1: Fitts' law parameters for four feedback conditions.**  
In Fitts' law, movement time is modeled as  $a + b \times ID$ . The index of performance is defined as the reciprocal of the slope, i.e.,  $1/b$ .

**Source for faster pointing.** We investigate the source of reduced completion times in active force-assisted conditions. Specifically, these improvements could be due to faster movements toward target under the attractive force field, or due to quicker selection enhanced by sensory feedback from the active force. We performed Post-hoc Tukey-Kramer tests to compare feedback conditions based on approach time (the duration from initial moving to the first entry into the target area), selection time (the remaining component of completion time) and entry count (the number of times the participant crosses the target boundaries).

Results show that all feedback conditions differ significantly in terms of overall completion time ( $p < 0.001$ ). However, the most pronounced differences are observed in selection time, where all pairwise comparisons yield a high significant difference level  $p < 0.001$ , as illustrated in Fig. 7a. In contrast, the differences in approach time are less significant ( $p < 0.05$ ) or not significant (e.g. *vision* vs *active force*) (except *vision* vs *vision + active force* where

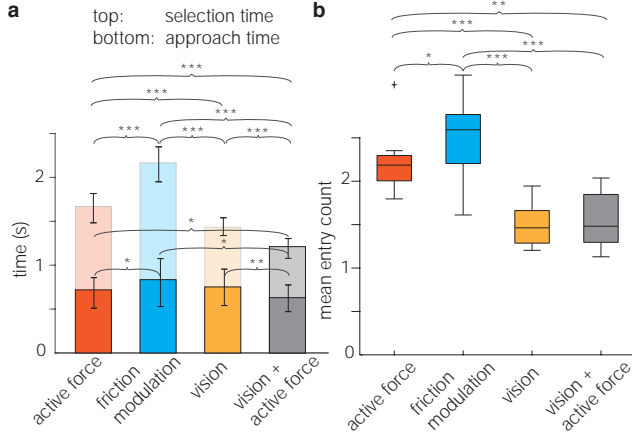


**Figure 7:** (a) The completion time of a pointing task comprises two components: approach time (dark-colored bar at the bottom) and selection time (light-colored bar at the top). (b) Box plot of entry count for each feedback condition. Stars indicate the significance level: \*  $p < 0.05$ , \*\*  $p < 0.01$  and \*\*\*  $p < 0.001$

$p < 0.01$ ). The variation in selection time is partially supported by participants' sliding behavior. Figure 7b reveals significant differences between haptic conditions: *active force* (mean = 2.17, SD = 0.8069) and *friction modulation* (mean = 2.41, SD = 1.03); between vision-present conditions: *vision* (mean = 1.47, SD = 0.60) and *vision + active force* (mean = 1.54, SD = 0.69), and no significant difference between *vision* and *vision + active force*. On average, the *active force* condition requires 0.237 fewer entry counts than *friction modulation*. This observation suggests that active force rendered target enhances user confidence by providing more compelling cues for target location.

**Subjective response.** Ten out of twelve participants provided feedback on their preferences and perceptions of the sensations. All ten participants expressed a clear preference for *active force* feedback over *friction modulation* for efficiently locating a target. They also described targets rendered with active force as having a "clear edge", whereas those by friction modulation felt like a "sticky region". Additionally, six participants noted a learning effect during both the training and experimental sessions. They commented that they initially moved cautiously to detect and identify the presence of a target but were able to move faster and more confidently after several minutes. This observation suggests that users' performance may improve with extended training.

## 6 Study 3: directional navigation

In this study, we investigate if suddenly activating a potential field under a stationary finger communicate a directional cue to users and help them navigate toward the target.

### 6.1 Study design

We deployed a pointing task using the GUI where the start area was located at the center, as shown in Fig. 8. We used a repeated within-subjects design with three independent variables: feedback

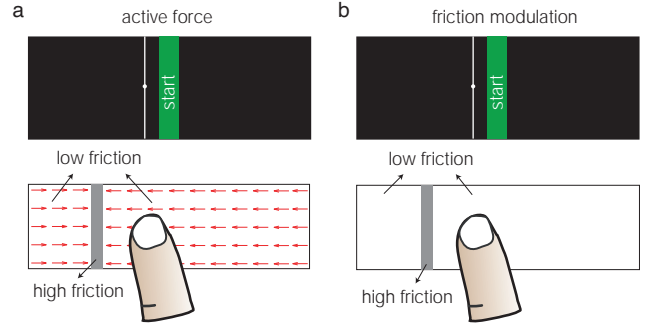


**Figure 8:** Top: GUI of a pointing task with directional navigation. The invisible target can locate to the right or left of the start area. Bottom: force or friction field in *active force* (a) or *friction modulation* (b) condition, respectively.

conditions, target widths, and target distances. Feedback conditions were *active force* and *friction modulation*. The force and friction profiles are presented in Fig. 8. Target distance to the start area were  $\pm 250$  pixels and  $\pm 350$  pixels, and target widths were 16 pixels and 32 pixels.

During the experiments, participants first placed their index finger on the start area, where no tactile feedback was provided. Once the active force or friction modulation profile issued, they started the pointing task. They were encouraged to use the directional cues to facilitate target searching.

**Participants.** Ten participants (5 females and 5 males, aged 21–28, all right-handed) were recruited for this study. All reported no sensory impairments or skin ailments. None participated in S1–2.

## 6.2 Results

RM-ANOVA on completion time reveals a statistically significant effect of feedback conditions ( $F_{1,9} = 92$ ,  $p = 5.1 \times 10^{-6}$ ), and target widths ( $F_{1,9} = 9.4$ ,  $p = 0.014$ ), but no significant effect of target distances ( $F_{1,9} = 0.055$ ,  $p = 0.82$ ). Post-hoc comparisons show a significant difference between *active force* and *friction modulation* in all the four movement conditions ( $p < 0.001$ ), as shown in the box plots of completion times in Figure 9a. On average, *active force* leads to a considerably shorter completion time compared to *friction modulation* (1.82 s vs. 3.10 s), reflecting a 41.26% reduction. This improvement is even more significant than the 22.9% reduction observed in S2.

To identify the source of this reduction, we analyzed the error rates in participants' initial moving direction. The friction modulation condition exhibited a considerably higher error rate of 51%, close to random choice. By contrast, the error rate in *active force* condition was only 12%, demonstrating that active force feedback provides salient directional cues.

Movement trajectories further highlight the difference in participants' selection behavior in these two feedback conditions. For a condition where the target width is 16 pixels and the distance is 350 pixels, trajectories in *active force* show a clear bias towards the target side. Conversely, trajectories under *friction modulation* were more evenly distributed between both directions (Fig. 10).

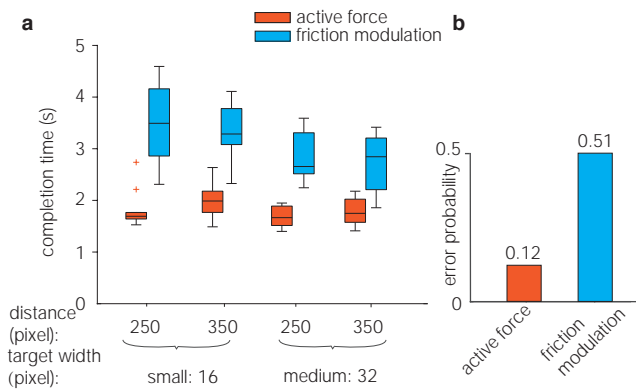


**Figure 9: (a) Mean completion time in a pointing task with directional navigation. (b) The error rate in terms of correctly moving to the target side upon the onset of active force or friction modulation activation.**

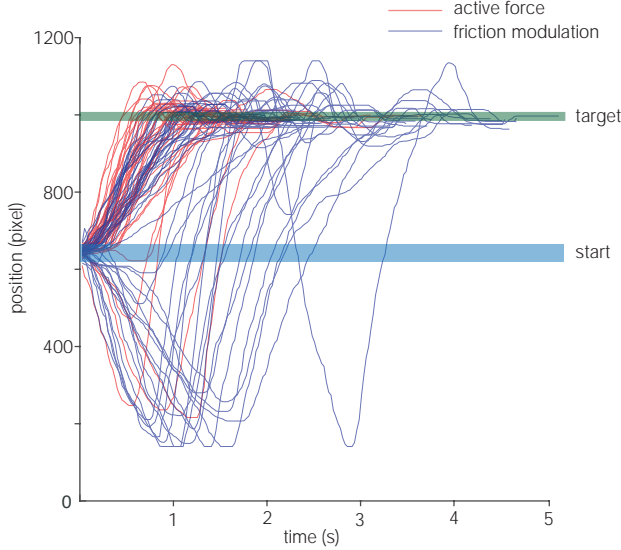


**Figure 10: Trajectories in a pointing task with directional navigation where the target width is 16 pixels and the target distance is 350 pixels. Red: active force condition; blue: friction modulation condition.**

These biased trajectories and the lower error rate indicate that the directional force field effectively directed the users toward lower potential, resulting in shorter completion times.

## 7 User experience with applications

Here, we showcase three applications to demonstrate the role of potential fields in enhancing touch interaction tasks. The designed potential fields in these applications correspond to those in S1-3. For each application, we outline the motivation behind its design,

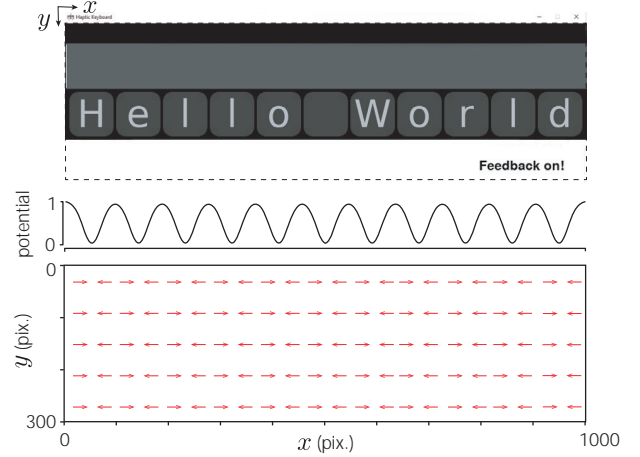


**Figure 11: Design of a virtual keyboard rendered by Gaussian potential wells. From top to bottom is the graphical user interface, potential function regarding x and the force field.**

detail its implementation, and evaluate user experience based on subjective responses.

### 7.1 Application design

**Haptic Keyboard.** Typing on a featureless touchpad or touch-screen requires users to visually search for keys and avoid clicking on incorrect locations (e.g. between keys). This process is significantly slower and more visually demanding compared to typing on a physical keyboard, where muscle memory enables effortless key localization. The potential field approach can be suitable to help users navigate to the desired keys on a virtual keyboard.

Here, we create attractive potential fields centered in the middle of each key, similar to those evaluated in the psycho-physical study in S1. The overall potential field on the surface is the sum of these individual potentials, as shown in Fig. 11. The exemplar displays the text "Hello World" to showcase how haptic feedback guide users in locating and sliding to keys. In practical applications, this approach can be customized to support various layouts, such as the standard "QWERTY" configuration. Additionally, it can be integrated with key-click sensation, as described in [8], to restore both the key localization and key press functions. We will examine whether these potential fields can improve users' ability to locate keys and avoid clicking on wrong keys.

**Three-Digit Lock.** The Three-Digit Lock game was created to assess whether users can locate a "password", using only tactile feedback, as illustrated in Fig. 12. In this game, users discover a randomly generated three-digit password by sliding on the touchpad to rotate the dials in each row. The design incorporates a directional step-wise force field, similar to that in S3. The "valley" of the attractive potential field corresponds to the location of the password on the dial. The step-change force around a sticky region is implemented to assist users in locating the correct digit effectively.

**Angry Birds Game.** An attractive potential field was designed to replicate the pulling sensation of a slingshot. Within the maximum stretchable length of the slingshot, the force vector linearly increases with the length. Beyond this limit, the lateral force plateaus.

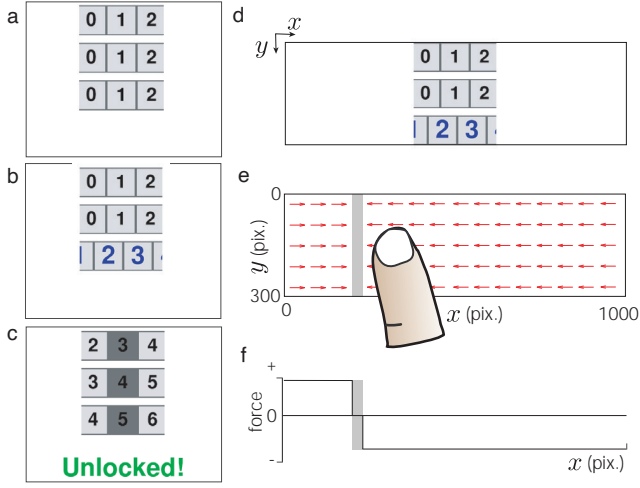


**Figure 12: A three-digit lock game that facilitates password finding using step-wise attractive force fields.**

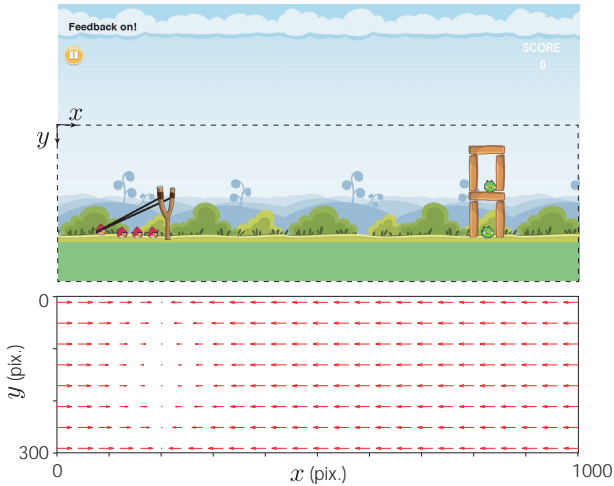


**Figure 13: Angry Birds Game in which the slingshot creates an attraction field. The lateral force is proportional to the distance to the slingshot.**

Once the user catches the slingshot, they can perceive both the intensity and direction of the dragging forces, even when stationary.

## 7.2 User study and results

**Experimental Procedures.** Participants interacted with each of the three applications for three minutes, then completed a comparison questionnaire and answered three open-ended questions. During the interaction, they were encouraged to toggle the haptic feedback on and off to compare the potential fields with the plain aluminum surface. The presentation order of the applications followed a Latin Square design to minimize ordering effects.

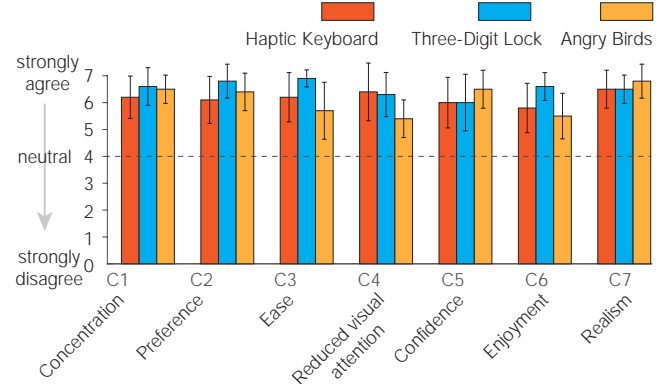


**Figure 14: Mean and standard deviation of ratings from the comparison questionnaire (C1 to C7) for Haptic Keyboard, Three-Digit Lock, and Angry Birds.**

The comparison questionnaire, adapted from Levesque et al. [21], assessed the effects of potential fields in seven dimensions: concentration, preference, ease of use, reduced visual load, realism, confidence, and enjoyment. Participants rated each aspect on a 7-point Likert scale (from "strongly disagree" to "strongly agree"). The statements were:

- C1. Concentration: Compared to no feedback, tactile feedback made me more focused and absorbed in the interaction task.
- C2. Preference: I prefer tactile feedback over no feedback.
- C3. Ease: Tactile feedback made the task easier to perform.
- C4. Reduced visual attention: Tactile feedback reduced my need for visual attention.
- C5. Realism: The interaction felt more realistic with tactile feedback.
- C6. Confidence: With tactile feedback, I felt more confident in my movements and actions.
- C7. Enjoyment: Tactile feedback made the application more enjoyable.

The three open-ended questions for each application were:

- Q1: How would you describe the sensations of tactile feedback in this application?
- Q2: Is there anything you liked or disliked about tactile feedback?
- Q3: Do you have any suggestions on how the sensations could be improved?

**Participants.** We recruited ten participants (five females), aged 22 to 43. One was left-handed, and nine were right-handed. None participated in previous sessions (S1–3).

**Results.** Figure 14 presents the average ratings and standard deviations for each question (C1 to C7) across three applications. All averaged ratings across participants of each question and application are positive (above 4, or "Neutral"), indicating favorable feedback from participants.

The **Haptic Keyboard** received the highest score in C4 (reduced visual attention), with an average of 6.4. Participants noted that

the tactile feedback helped them locate their fingers on the keys without the need of visual confirmation. For example, P5 remarked, *"It made it easier to feel the location of my fingers on the keyboard without looking at it."* and *"The distance between keys is similar to my keyboard, so I could move my finger fast."* P1 commented, *"It confirmed I was in the right spot on the keys, not between them."* Some participants described the sensation as *"like playing with magnets"* (P7) or *"like surfing on the surface, but not like a mechanical keyboard"* (P6).

The **Three-Digit Lock** ranked highest in C1, C2, C3, and C6 (concentration, preference, ease, and confidence). Participants reported that they could find the correct password within seconds after starting searching. They frequently mentioned that the feedback made it easy to locate the correct password, with P2-P9 describing the sensation of reaching to the password as *"very clear."*

The **Angry Birds Game** scored highest in C5 (realism) and C7 (enjoyment). Participants frequently mentioned a strong sense of realism and fun in Q1 and Q2. Comments included *"I felt like I was dragging a rubber band"* (P6) and *"a slingshot"* (P10). P10 also stated, *"I could clearly feel that the more I dragged, the more force was pulling my finger."*

Negative feedback and suggestions for improvement were collected in Q2 and Q3. For the Angry Birds Game, P10 noted, *"Sometimes I couldn't feel the change in force when I pulled the slingshot further."* For the haptic keyboard, P2 mentioned, *"The force feedback was disappointing when I wasn't in the middle of a key"*, while P5 suggested, *"It would be great if the keyboard worked in two dimensions"*. P10 proposed integrating *"a key-click sensation"* for enhanced realism."

## 8 Discussion

Advances in active force-based surface haptics have shown the potential to add a new dimension to tactile feedback. However, prior research has primarily focused on hardware development. In this study, we implemented programmable impedance control by real-time modulating traveling wave parameters and designed several user studies to evaluate its effectiveness. For the first time, we demonstrate the positive impact of active force feedback in users during sliding interaction, supported by both measurable performance gains and positive user experience.

Three HCI applications received positive feedback from participants, further confirming the transferability of these benefits observed in S1-3 to practical use cases. These findings could inspire more applications and tactile interface design. Next, we discuss some implications of these results, assess their values, and address the limitations and recommendations for future research.

### 8.1 Haptic guidance with potential fields

The artificial Potential Field method is widely used in classical haptics and robotic applications, such as haptic rendering for training [28] and teleoperation [20] and path planning for mobile robots [35]. This method generates repulsive fields for obstacle avoidance and attractive fields for path guidance. To display potential fields on a flat surface, the necessity is to have active forces that can build up potential. We successfully implemented programmable surface potential field rendering by controlling traveling waves in real time.

Importantly, we have three key observations in users: they have a clear awareness of the scale and polarity of these potentials, they show behavior change by being attracted to lower potential, and experience positive emotional effects.

It is valuable to compare friction modulation and active force feedback in haptic rendering. One can render 3D features by mapping the height of the feature directly to the friction [13], or by mapping the dot product of the sliding velocity and gradient of the feature to the local friction [18]. The resulting frictional field is a pseudo-potential field, due to the non-conservative nature of friction, thus only providing tactile cues on the sliding paths without indicating proximal features. As a result, this approach is often used to augment visually represented features [18], where the finger exploration is consciously guided by visual input. When visual feedback is absent or when the finger stops moving, the haptic guidance severely deteriorates. For example, in the case of guiding along a curved path in Fig. 2c, users have to slide back and forth around the path to identify it, and path following becomes inaccurate and time-consuming. In contrast, active forces can create both repulsive and attractive fields that can push the finger to the path effectively and robustly, even without a need for visual input.

Unlike other haptic devices that provide directional guidance through handheld tools, such as tactile compasses [22] or pseudo-forces [26], our approach enables bare-finger interaction by instrumenting a surface with traveling waves. Users can freely use their fingers for other tasks and engage with the guidance only when desired. This feature might be well-suited for integration into haptic touchpads, screen readers for visually impaired users, large touchscreens in vending machines or museum exhibits, and educational displays. These applications can facilitate touch interactions and simulate physics like flowing fluids, or elastic springs.

### 8.2 Pointing facilitation using active force vs friction modulation

In the pointing task in S2, augmenting the high-friction target with active forces led to a significant permanence gain of 22.9%, compared to the friction modulation approach using the same level of actuation. This improvement does not appear to arise from faster approach but rather from enhanced target awareness, as evidenced by the observations of variation in selection duration, sliding behavior, and participants' descriptions of their target perception.

Indeed, when we look at target rendering from the perspective of a fingertip, it undergoes a temporal evolution of tactile stimuli during reaching. In the active force scheme, the finger experiences a sudden change in impedance, that is from a negative impedance (i.e. pushing forces) to positive impedance (high friction and resisting force). In contrast, friction modulation scheme only involves a sudden increase in friction. This additional reversal of the active lateral force enhances the "braking" effect upon reaching the target, making it easier for the finger to stop near the target.

This advantage is particularly evident for rendering small targets. Due to inertia, the finger may continue sliding upon entering the target area. The friction modulation approach only generates a short duration that users can feel a high friction. This short-lived feeling of high impedance may well be insufficient to trap the finger

or even aware users. Consequently, users may miss the target and need to slide back and forth to identify it. This limitation leads to a marked performance degradation. For instance, reaching a small target (width = 1.6 mm) with friction modulation requires 30.94% more time compared to larger targets. In contrast, active forces still possess an abrupt change of lateral force, no matter how small the target is, resulting in reduced degradation due to small target of 18.51%. This feature offers higher rendering resolution, making active force feedback especially suitable for rendering small elements, such as text.

### 8.3 Possibility to restore procedural memory

While we did not statistically investigate learning effects in this paper, we did observe variable learning among participants during the training and experimental sessions. In S2, some participants reported noticeable performance improvements in the training, as indicated in their verbal feedback. This improvement is also reflected in their adapted targeting behavior. In some trials, they first performed a fast-reaching movement to quickly estimate the target location and then used more controlled movements to finely locate the target. This strategy resulted in larger overshoots but shorter completion times. These observations indicate the development of procedural memory in users through leveraging tangible potential fields.

We anticipate that further improvements in performance could be achieved with continued learning. In our experimental design, feedback conditions were randomized across trials, and participants were unaware of the specific conditions they would encounter prior to each trial. Consequently, they were unable to fully exploit the procedural memory that could have been developed. In practical applications where haptic feedback conditions are predetermined, users could build procedural memory more effectively. This would enable them to employ their learned muscle memory with greater confidence, potentially leading to even faster and more efficient target selections. Moreover, when integrating this haptic-assisted pointing with keyclick sensations [7, 8, 17, 39], it is promising to achieve eyes-free control over virtual widgets, benefiting sighted users in visually demanding situations and allowing visually impaired users to access them.

### 8.4 Limitations and future work

We acknowledge several limitations in this work. First, we did not address the variability in the perceived intensity of stimuli. The apparatus operates in feed-forward. Different pressing forces and fingertip stiffness can cause variable force output between individuals and trials. Second, the force generation model did not consider sliding velocity. We used a data-driven force-phase model, measured with a static finger. Fast and slow-moving fingers may result in different actual force output. These limitations could be addressed by incorporating closed-loop control to monitor and adjust force output.

Furthermore, future work could be extended to the following directions:

**Expanding interaction modalities.** Future work could explore more interaction modalities using potential fields, such as improving Steering Law tasks or guiding users along curved paths without visual feedback.

**Broader application design.** More potential fields could be tailored to specific applications, such as rendering racetrack lanes in racing games, creating tactile chessboard grids, or adding periodic potential wells that fit bookmark bars of a computer or fit contents to be scrolled on touchscreens.

**Two-dimensional active force feedback SHD.** To date, only one-dimensional active force feedback SHDs are documented in the literature. This work reveals the pressing need for two-dimensional active force SHDs that generates lateral forces in any direction on a surface. The demonstrated benefits of the potential field approach in this paper could be directly extended to two-dimensional applications.

## 9 Conclusion

We created artificial potential fields on the fingertip by dynamically adjusting the traveling wave ratio in an active force SHD. These potentials significantly enhanced touch interaction in three tasks: (1) perception of bumps and holes, (2) Fitts' pointing tasks, and (3) directional navigation. User studies qualitatively demonstrated that the generated potential fields effectively convey both the height and depth of the fields and guide the finger toward targets.

We designed three applications to showcase the versatility of potential field design. These applications leverage the strengths of the aforementioned qualitative studies. User feedback confirmed that these applications are well-suited for incorporating these haptic renderings. Our findings highlight that rendering potential fields by controlling traveling waves is an effective way to guide bare finger interactions with touch alone. This capability is only possible with active force feedback and cannot be replicated with vibrotactile or friction modulation techniques. This research underscores the promise of artificial potential field rendering to enhance touch interactions and provide diverse and immersive tactile experiences.

## Acknowledgments

The work of ZC was supported by China Scholarship Council under Grant 202006320048. MW acknowledges the support of the NWO VIDI project 19680.

## References

- [1] Ugur Alican Alma, Gholamreza Ilkhani, and Evren Samur. 2016. On Generation of Active Feedback with Electrostatic Attraction. In *Haptics: Perception, Devices, Control, and Applications (Lecture Notes in Computer Science)*, Fernando Bello, Hiroyuki Kajimoto, and Yon Visell (Eds.). Springer International Publishing, Cham, 449–458. [https://doi.org/10.1007/978-3-319-42324-1\\_44](https://doi.org/10.1007/978-3-319-42324-1_44)
- [2] Mehmet Ayyildiz, Michele Scaraggi, Omer Sirin, Cagatay Basdogan, and Bo N. J. Persson. 2018. Contact mechanics between the human finger and a touchscreen under electroadhesion. *Proc. Nat. Acad. Sci.* 115, 50 (Dec. 2018), 12668–12673. <https://doi.org/10.1073/pnas.1811750115>
- [3] Mirai Azechi and Shogo Okamoto. 2023. Easy-to-recognize bump shapes using only lateral force cues for real and virtual surfaces. In *2023 IEEE World Haptics Conference (WHC)*. IEEE, IEEE, Delft, Netherlands, 397–402. <https://doi.org/10.1109/WHC56415.2023.10224399>
- [4] Olivier Bau, Ivan Poupyrev, Ali Israr, and Chris Harrison. 2010. TeslaTouch: electrovibration for touch surfaces. In *Proceedings of the 23rd annual ACM symposium on User interface software and technology (UIST '10)*. Association for Computing Machinery, New York, NY, USA, 283–292. <https://doi.org/10.1145/1866029.1866074>

[5] Corentin Bernard, Jocelyn Monnoyer, Solvi Ystad, and Michael Wiertlewski. 2022. Eyes-Off Your Fingers: Gradual Surface Haptic Feedback Improves Eyes-Free Touchscreen Interaction. In *Proceedings of the 2022 CHI Conference on Human Factors in Computing Systems (CHI '22)*. Association for Computing Machinery, New York, NY, USA, 1–10. <https://doi.org/10.1145/3491102.3501872>

[6] Mélisande Biet, Frédéric Giraud, François Martinot, and Betty Semail. 2006. A Piezoelectric Tactile Display Using Travelling Lamb Wave. In *Proceedings of Eurohaptics*. Paris, France, 567–570.

[7] Detjon Brahimaj, Mondher Ouari, Anis Kaci, Frédéric Giraud, Christophe Giraud-Audine, and Betty Semail. 2023. Temporal Detection Threshold of Audio-Tactile Delays With Virtual Button. *IEEE Transactions on Haptics* 16, 4 (Oct. 2023), 491–496. <https://doi.org/10.1109/TOH.2023.3268842>

[8] Zhaochong Cai and Michał Wiertlewski. 2023. UltraLoop: Active lateral force feedback using resonant traveling waves. *IEEE Transactions on Haptics* 16, 4 (2023), 652–657. <https://doi.org/10.1109/TOH.2023.3276590>

[9] Géry Casiez, Nicolas Roussel, Romuald Vanbelleghem, and Frédéric Giraud. 2011. SurfPad: riding towards targets on a squeeze film effect. In *Proceedings of the SIGCHI Conference on Human Factors in Computing Systems (CHI '11)*. Association for Computing Machinery, New York, NY, USA, 2491–2500. <https://doi.org/10.1145/1978942.1979307>

[10] Changhyun Choi, Yuan Ma, Xinyi Li, Sitangshu Chatterjee, Sneha Sequeira, Rebecca F Friesen, Jonathan R Felts, and M Cynthia Hipwell. 2022. Surface haptic rendering of virtual shapes through change in surface temperature. *Science Robotics* 7, 63 (2022), eabl4543. <https://doi.org/10.1126/scirobotics.abl4543>

[11] Erik C. Chubb, J. Edward Colgate, and Michael A. Peshkin. 2010. ShiverPad: A Glass Haptic Surface That Produces Shear Force on a Bare Finger. *IEEE Trans. Haptics* 3, 3 (July 2010), 189–198. <https://doi.org/10.1109/TOH.2010.7>

[12] Xiaowei Dai, J. Edward Colgate, and Michael A. Peshkin. 2012. LateralPaD: A surface-haptic device that produces lateral forces on a bare finger. In *2012 IEEE Haptics Symposium (HAPTICS)*. IEEE, Vancouver, BC, Canada, 7–14. <https://doi.org/10.1109/HAPTIC.2012.6183753>

[13] DS Ebert. 2002. *Texturing & Modeling, A procedural Approach*. Morgan Kaufman, San Francisco, CA, USA.

[14] Pierre Garcia, Frédéric Giraud, Betty Lemaire-Semail, Matthieu Rupin, and Michel Amberg. 2020. 2MoTAC: Simulation of Button Click by Superposition of Two Ultrasonic Plate Waves. In *Haptics: Science, Technology, Applications*. Springer International Publishing, Leiden, The Netherlands, 343–352. [https://doi.org/10.1007/978-3-030-58147-3\\_38](https://doi.org/10.1007/978-3-030-58147-3_38)

[15] Eloïsa Garcia-Canseco, Alain Ayemlong-Fokem, Alex Serrarens, and Maarten Steinbuch. 2010. Haptic Simulation of a Gear Selector Lever Using Artificial Potential Fields. *IFAC Proceedings Volumes* 43, 13 (Jan. 2010), 426–429. <https://doi.org/10.3182/20100831-4-FR-2021.00075>

[16] Sofiane Ghenna Eric Vezzoli, Christophe Giraud-Audine, Frederic Giraud, Michel Amberg, and Betty Lemaire-Semail. 2017. Enhancing Variable Friction Tactile Display Using an Ultrasonic Travelling Wave. *IEEE Trans. Haptics* 10, 2 (2017), 296–301. <https://doi.org/10.1109/TOH.2016.2607200>

[17] David Gueorguiev, Anis Kaci, Michel Amberg, Frédéric Giraud, and Betty Lemaire-Semail. 2018. Travelling Ultrasonic Wave Enhances Keyclick Sensation. In *Haptics: Science, Technology, and Applications*. Springer International Publishing, Pisa, Italy, 302–312. [https://doi.org/10.1007/978-3-319-93399-3\\_27](https://doi.org/10.1007/978-3-319-93399-3_27)

[18] Seung-Chan Kim, Ali Israr, and Ivan Poupyrev. 2013. Tactile rendering of 3D features on touch surfaces. In *Proceedings of the 26th annual ACM symposium on User interface software and technology (UIST '13)*. Association for Computing Machinery, New York, NY, USA, 531–538. <https://doi.org/10.1145/2501988.2502020>

[19] Emilia Koskinen, Topi Kaaresoja, and Pauli Laitinen. 2008. Feel-good touch: finding the most pleasant tactile feedback for a mobile touch screen button. In *Proceedings of the 10th international conference on Multimodal interfaces (ICMI '08)*. Association for Computing Machinery, New York, NY, USA, 297–304. <https://doi.org/10.1145/1452392.1452453>

[20] Thanh Mung Lam, Harmen Wigert Boschloo, Max Mulder, and Marinus M. van Paassen. 2009. Artificial Force Field for Haptic Feedback in UAV Teleoperation. *IEEE Transactions on Systems, Man, and Cybernetics - Part A: Systems and Humans* 39, 6 (Nov. 2009), 1316–1330. <https://doi.org/10.1109/TSMCA.2009.2028239>

[21] Vincent Levesque, Louise Oram, Karon MacLean, Andy Cockburn, Nicholas D. Marchuk, Dan Johnson, J. Edward Colgate, and Michael A. Peshkin. 2011. Enhancing physicality in touch interaction with programmable friction. In *Proceedings of the SIGCHI Conference on Human Factors in Computing Systems (CHI '11)*. Association for Computing Machinery, Vancouver BC, Canada, 2481–2490. <https://doi.org/10.1145/1978942.1979306>

[22] Guanhong Liu, Tianyu Yu, Chun Yu, Haiqing Xu, Shuchang Xu, Ciyan Yang, Feng Wang, Haipeng Mi, and Yuanchun Shi. 2021. Tactile Compass: Enabling Visually Impaired People to Follow a Path with Continuous Directional Feedback. In *Proceedings of the 2021 CHI Conference on Human Factors in Computing Systems (CHI '21)*. Association for Computing Machinery, New York, NY, USA, 1–13. <https://doi.org/10.1145/3411764.3445644>

[23] Joe Mullenbach, Dan Johnson, J. Edward Colgate, and Michael A. Peshkin. 2012. ActivePaD surface haptic device. In *2012 IEEE Haptics Symposium (HAPTICS)*. IEEE, Vancouver, BC, Canada, 407–414. <https://doi.org/10.1109/HAPTIC.2012.6183753>

[24] Joseph Mullenbach, Michael Peshkin, and J. Edward Colgate. 2017. eShiver: Lateral Force Feedback on Fingertips through Oscillatory Motion of an Electroadhesive Surface. *IEEE Trans. Haptics* 10, 3 (July 2017), 358–370. <https://doi.org/10.1109/TOH.2016.2630057>

[25] Reza Haghghi Osgouei, Jin Ryong Kim, and Seungmoon Choi. 2017. Improving 3D Shape recognition with electrostatic friction display. *IEEE transactions on haptics* 10, 4 (2017), 533–544. <https://doi.org/10.1109/TOH.2017.2710314>

[26] Jun Rekimoto. 2014. Traxion: a tactile interaction device with virtual force sensation. In *ACM SIGGRAPH 2014 Emerging Technologies (SIGGRAPH '14)*. Association for Computing Machinery, New York, NY, USA, 1. <https://doi.org/10.1145/2614066.2614079>

[27] Jing Ren, Kenneth A. McIsaac, Rajni V. Patel, and Terry M. Peters. 2007. A Potential Field Model Using Generalized Sigmoid Functions. *IEEE Transactions on Systems, Man, and Cybernetics, Part B (Cybernetics)* 37, 2 (April 2007), 477–484. <https://doi.org/10.1109/TCMB.2006.883866>

[28] Jing Ren, Rajni V. Patel, Kenneth A. McIsaac, Gerard Guiraudon, and Terry M. Peters. 2008. Dynamic 3-D Virtual Fixtures for Minimally Invasive Beating Heart Procedures. *IEEE Transactions on Medical Imaging* 27, 8 (Aug. 2008), 1061–1070. <https://doi.org/10.1109/TMI.2008.917246>

[29] Louis B. Rosenberg. 1993. Virtual fixtures as tools to enhance operator performance in telepresence environments. In *Telemanipulator technology and space telerobotics*, Vol. 2057. SPIE, IEEE, Seattle, WA, USA, 10–21. <https://doi.org/10.1109/VRAIS.1993.380795>

[30] Anne Roudaut, Andreas Rau, Christoph Sterz, Max Plauth, Pedro Lopes, and Patrick Baudisch. 2013. Gesture output: eyes-free output using a force feedback touch surface. In *Proceedings of the SIGCHI Conference on Human Factors in Computing Systems (CHI '13)*. Association for Computing Machinery, New York, NY, USA, 2547–2556. <https://doi.org/10.1145/2470654.2481352>

[31] Satoshi Saga and Koichiro Deguchi. 2012. Lateral-force-based 2.5-dimensional tactile display for touch screen. In *2012 IEEE Haptics Symposium (HAPTICS)*. IEEE, Vancouver, BC, Canada, 15–22. <https://doi.org/10.1109/HAPTIC.2012.6183764>

[32] K. Salisbury, D. Brock, T. Massie, N. Swarup, and C. Zilles. 1995. Haptic rendering: programming touch interaction with virtual objects. In *Proceedings of the 1995 symposium on Interactive 3D graphics (I3D '95)*. Association for Computing Machinery, New York, NY, USA, 123–130. <https://doi.org/10.1145/199404.199426>

[33] W. Seemann. 1996. A linear ultrasonic traveling wave motor of the ring type. *Smart Material Structure* 5, 3 (June 1996), 361–368. <https://doi.org/10.1088/0964-1726/5/3/015>

[34] Craig D. Shultz, Michael A. Peshkin, and J. Edward Colgate. 2015. Surface haptics via electroadhesion: Expanding electrovibration with Johnsen and Rahbek. In *2015 IEEE World Haptics Conference (WHC)*. IEEE, Evanston, IL, USA, 57–62. <https://doi.org/10.1109/WHC.2015.7177691>

[35] P. Vadakkepat, Kay Chen Tan, and Wang Ming-Liang. 2000. Evolutionary artificial potential fields and their application in real time robot path planning. In *Proceedings of the 2000 Congress on Evolutionary Computation. CEC00 (Cat. No.00TH8512)*, Vol. 1. IEEE, La Jolla, CA, USA, 256–263 vol.1. <https://doi.org/10.1109/CEC.2000.870304>

[36] T. Watanabe and S. Fukui. 1995. A method for controlling tactile sensation of surface roughness using ultrasonic vibration. In *Proceedings of 1995 IEEE International Conference on Robotics and Automation*, Vol. 1. IEEE, Nagoya, Japan, 1134–1139. <https://doi.org/10.1109/ROBOT.1995.525433>

[37] Michał Wiertlewski, F. Rebecca Fenton, and J. Edward Colgate. 2016. Partial squeeze film levitation modulates fingertip friction. *Proc. Nat. Acad. Sci.* 113, 33 (Aug. 2016), 9210–9215. <https://doi.org/10.1073/pnas.1603908113>

[38] Laura Winfield, John Glassmire, J. Edward Colgate, and Michael Peshkin. 2007. T-PaD: Tactile Pattern Display through Variable Friction Reduction. In *Second Joint EuroHaptics Conference and Symposium on Haptic Interfaces for Virtual Environment and Teleoperator Systems (WHC'07)*. IEEE, Tsukuba, Japan, 421–426. <https://doi.org/10.1109/WHC.2007.105>

[39] Heng Xu, Roberta L. Klatzky, Michael A. Peshkin, and J. Edward Colgate. 2020. Localizable Button Click Rendering via Active Lateral Force Feedback. *IEEE Trans. Haptics* 13, 3 (July 2020), 552–561. <https://doi.org/10.1109/TOH.2020.2990947>

[40] Heng Xu, Michael A. Peshkin, and J. Edward Colgate. 2019. UltraShiver: Lateral Force Feedback on a Bare Fingertip via Ultrasonic Oscillation and Electroadhesion. *IEEE Trans. Haptics* 12, 4 (Oct. 2019), 497–507. <https://doi.org/10.1109/TOH.2019.2934853>

[41] Heng Xu, Michael A. Peshkin, and J. Edward Colgate. 2020. SwitchPaD: Active Lateral Force Feedback over a Large Area Based on Switching Resonant Modes. In *Haptics: Science, Technology, Applications*. Springer International Publishing, Leiden, The Netherlands, 217–225. [https://doi.org/10.1007/978-3-030-58147-3\\_24](https://doi.org/10.1007/978-3-030-58147-3_24)

[42] Yang Zhang and Chris Harrison. 2015. Quantifying the Targeting Performance Benefit of Electrostatic Haptic Feedback on Touchscreens. In *Proceedings of the 2015 International Conference on Interactive Tabletops & Surfaces (ITS '15)*. Association for Computing Machinery, New York, NY, USA, 43–46. <https://doi.org/10.1145/2817721.2817730>